Journal of Crystal Growth 487 (2018) 120–125

Contents lists available at ScienceDirect

Journal of Crystal Growth

journal homepage: www.elsevier.com/locate/crys

In-situ detection of convection and rotation striations by growth interface electromotive force spectrum

Yunzhong Zhu [a], Feng Tang [b], Xin Yang [b], Mingming Yang [b], Decai Ma [a], Xiaoyue Zhang [a], Yang Liu [a], Shaopeng Lin [a,*], Biao Wang [a,b,*]

[a] Sino French Institute of Nuclear Engineering and Technology, Sun Yat-sen University, Zhuhai 519082, China
[b] State Key Laboratory of Optoelectronic Materials and Technologies/Institute of Optoelectronic and Functional Composite Materials, School of Physics and Engineering, Sun Yat-sen University, Guangzhou 510275, China

ARTICLE INFO

Article history:
Available online 7 February 2018
Communicated by Lili Zheng

Keywords:
A2. Czochralski method
A1. Growth interface electromotive force
A1. Defects
A1. Convection
A1 Fluid flows
A1. Interfaces

ABSTRACT

Nanoscale growth striations, induced by the crystal rotation and melt convection, are in-situ detected by the growth interface electromotive force (GEMF) spectrum during Czochralski (CZ) crystal growth. Specifically, the intensity and period of rotation and convection striations could be precisely revealed under different rotation rates. This is because the GEMF spectrum is affected by the combination effort of temperature difference in crystal rotation path and the melt flow in growth interface. Furthermore, the spectrum analysis (Fourier transform) reveals remarkable characteristics of periodic flow oscillation. More interestingly, in different rotation rates, the corresponding convection period and intensity show particular regularity that could barely be observed in semitransparent and high-temperature melt. Therefore, the GEMF spectrum reflects the subtle changes of a growing crystal that is far beyond the detecting precision of sensors in current CZ equipment. On the basis of this paper and our previous work, the real-time feedback of multiscale striations is established. GEMF spectrum could be a promising approach to reveal striation formation mechanism and optimize crystal quality.

1. Introduction

Macroscopic single crystals are the pillar materials of industrial manufacture, medical facility and scientific research. In these sci-tech fields, the lingering obstacles to improve the crystal performance are defects that include point defects, dislocation, bubbles, segregation, growth striations, etc. Growth striations are widely known inherent and macro defects in single crystals [1]. They present the lattice distortion, inhomogeneous segregation, and even crack the crystalline. Because of the crucial role of growth striations to crystal quality, the development of artificial single crystals always keeps with the striations damping research [1–5]. It is known that growth striations are the result of the growth interface oscillatory movement due to the convective instability [6]. Thus, as a continuous and costly pursuit in crystal industry, a variety of technology had been offered to suppress the convection fluctuation: the adjustment of control parameters, magnetic field, ultrasound field, and accelerated crystal or crucible rotation technique (ACRT), for example [2–5]. However, since the lack of sensitive convection feedback, researchers could hardly obtain the effect of various striations adjustment approaches during the long-term crystal growth process. For optimizing the adjustment approaches and revealing the striations formation mechanisms, the in-situ detection of the melt convection and temperature fluctuation in growth interface is urgently needed.

In order to reveal the melt convection and temperature field in Czochralski (CZ) system, the indirect simulation experiments consisting of dummy crystal and hypothermal working fluids are offered [7–10]. Moreover, computer simulations present the corresponding convection characteristics as well [11–13]. These simulations reveal the basic hydromechanics issues of emulational CZ convection system. However, simulations tend to idealize the crystal growth condition, which generates certain differences between simulation result and realistic condition. Furthermore, different crucible shape, deficient thermal insulation, changing melt level and crystal boule, etc. complicate the growth condition. Thus, the specific convection condition of a growing crystal tends to be unpredictable. Besides, in realistic growth condition, the high-temperature melts may corrode contact sensors (thermocouples and flowmeters) [7]; and also, these contact sensors cannot reach the growth interface during crystal growth. Especially in $LiNbO_3$

* Corresponding authors at: Sino French Institute of Nuclear Engineering and Technology, Sun Yat-sen University, Zhuhai 519082, China (S.P. Lin and B. Wang).
E-mail addresses: lshpeng@mail.sysu.edu.cn (S. Lin), wangbiao@mail.sysu.edu.cn (B. Wang).

https://doi.org/10.1016/j.jcrysgro.2018.02.010
0022-0248/© 2018 Published by Elsevier B.V.

melts [14], the direct observation of horizontal temperature difference, periodic oscillatory flow, and corresponding growth striations are difficult [15].

In our previous work [16] an approach to in-situ reveal macroscopic thermal striations (0.5–1 mm width) has been established by detecting the growth interface electromotive force (GEMF, ϕ_{GE}) spectrum between crystal and melt. Benefiting from this method, thermal fluctuations are significantly weakened via the optimized growth parameters, and the corresponding macrostriations are eliminated. Then, using the atomic force microscopy (AFM), we further validate the smooth crystal surface of nanometers roughness. Such smooth surface could be roughly regarded as striations free production. However, on the surface, the regular striations of nanoscale height and micron-scale width are discovered by AFM and stereomicroscopy. In this paper, the striations generated in each lap of crystal rotation are defined as *rotation striations* [17] and the ones generated from the melt flow oscillation are called *convection striations* [18,19]. In the rotating growth interface of CZ system, the horizontal temperature difference consists of the unavoidable mechanical unbalance [20] and the inherent spoke pattern [21] of the melt surface. The vertical interval of rotation striations simply depends on the growth rate (v) and the rotation period. On the other hand, the melt flow oscillation is an inherent characteristic of CZ convection systems [19], which is mainly produced by the buoyant force (natural convection) and the crystal rotation (forced convection) [22]. In CZ melt, the competition of buoyancy and crystal rotation generates a typical fluid dynamics phenomenon of baroclinic instability, which results in periodic convection oscillation [23]. Thus, in different rotation rates, the corresponding convection period and intensity show particular regularity.

We have known that the GEMF can depict the crystallization, transport and segregation of ionic species in $LiNbO_3$ melt [24,25]. The outstanding detectability owes to its composition. Specifically, the GEMF consists of crystallization electromotive force (CEMF) and the thermoelectromotive force [16,24]. The CEMF is generated from the partitioning of oppositely charged valence ions on both sides of the growth interface, and the thermoelectromotive force consists of the supercooling electromotive force (SEMF) in growth interface and the Seebeck potential between crystal and melt [25]. To be specific, Seebeck potential is mainly related to the pulling height and contributes to the slope of GEMF. Besides the slope factor, CEMF and SEMF relate with the crystal growth rate and the temperature of growth interface [16]. Therefore, the fluctuation of GEMF spectrum reflects the transient and periodic temperature and the convection variation of growth interface. It is worth noting that the GEMF fluctuation reveals the variation of the exact crystal-melt interface that a thermocouple cannot reach. Growth interface is the core position of a growing crystal and the region to form striations as well. Thus, using the GEMF spectrum, the rotation and convection oscillation in growth interface could be revealed in situ, respectively.

As mentioned above, the rotation and convection striations are induced by the external factor of melt temperature difference and the inherent factor of melt flow oscillation. Furthermore, our GEMF experiments present that, in different rotation rates the corresponding convection period and intensity show particular characteristics. To elaborate on the particular characteristics, the performance of rotation and convection are systematically discussed in two extreme cases of low and high rotation rates. The striations in low and high rotation rates are found to be rotation dominant and convection dominant, respectively; and the regular distributions of both kinds of striations are the corresponding external expression. Thus, GEMF spectrum performs far beyond the detecting precision of existing crystal growth sensors. The more remarkable thing is that, it offers a real-time feedback of convection suppression approaches to enhance crystal quality and could be used to reveal striations formation mechanism as well.

2. Materials and methods

2.1. Single crystal growth

The raw material of congruent lithium niobate (LN) is consist of 48.6 mol% Li_2CO_3 (99.99% purity) and 51.4 mol% Nb_2O_5 (99.99% purity) powders. The raw mixture was mixed and ball milled with three times of their weight in high-purity urea, then synthesized by a solid-state combustion route [26] in 700 °C. After that, LN crystals were grown by the full-automatic CZ equipment. It is worth mentioning that the thermal insulation of crystal growth is the same as our previous work. Thus, the similar temperature field guarantees the predictable crystal growth electromotive force function of growth rate, $\phi^{growth}(v)$ [16].

2.2. GEMF system description

During crystal growth process, the GEMF in different rotation rates (n) was captured between the platinum crucible and the pulling rod by a Keithley 2100 multimeter (as presented in Fig. 1). To achieve more precise and sensitive GEMF feedback, the sampling rate was upgraded to 10 Hz. Therefore, the transient and regular GEMF variation of crystal rotation and convection oscillation could be obtained. In order to further analysis the GEMF spectrum, the fast Fourier transform (FFT) and the window function of Hanning were used. Thus, the FFT power spectrum of mean squared amplitude (Power as MSA) can be used to distinguish the main frequency and the proportion of rotation and convection oscillation accurately. Each GEMF spectrum of specific rotation rate contains the time interval of 1800 s, which ensures the sufficient data accuracy of MSA spectrum. In addition, since the GEMF is obtained with a constant pulling rate, the Seebeck effect will generate a constant slope in GEMF spectrum. Obviously, the slope factor will be presented as a peak of ultra-low frequency and sky-high amplitude in MSA spectrum. Therefore, in order to reveal the crystal rotation and melt convection frequency, the low frequency of the slope should be filtered out.

2.3. Striations morphology characterization

The striations on the surface of as-grown crystals were shot by a stereomicroscopy (Nikon SZM18) and an AFM (Asylum Research MFP-3D Infinity). It is known that the crystal surface is not an ideal

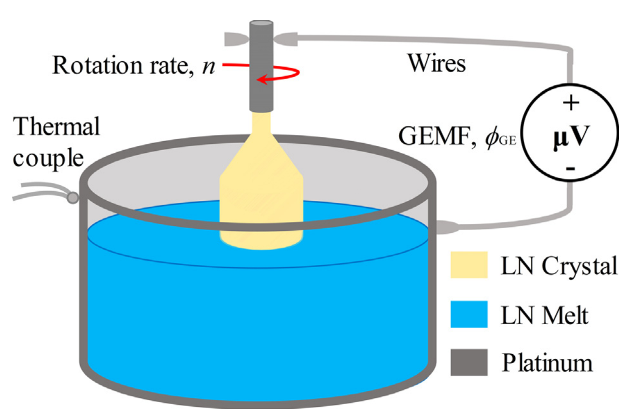

Fig. 1. Schematic of the experimental platform. The GEMF (ϕ_{GE}) between the solid crystal and melt in various rotation rates is captured by a multimeter.

plane (the radial arc convex and the axial diameter variation), and therefore, the curving surface may weaken the image sharpness of stereomicroscopy. The fine scanning of AFM could make up the deficiency of microscopy, but its limited scanning width of 90 μm cannot depict the striations of broad vision. In consequence, the complementation of stereomicroscopy and AFM could reveal the general and the fine striations morphology, simultaneously. These striations distribution can verify the GEMF spectrum analysis. Hence, combining with GEMF analysis, the specific performance of micro-striations will be discussed in details as follows.

3. Results and discussion

Benefiting from our previous study on GEMF spectrum [16], we achieved the in-situ detection of macro-striations and attributed the macro-striations to the feeble output power fluctuation. When we further obtained the constant power factor and upgraded the sampling rate of data record, interestingly, the rotation frequency (f_R) and the subtle convection frequency (f_C) were observed in GEMF spectrum.

3.1. GEMF of rotation striations

Rotation striations are common phenomenon of single crystals and are formed in each rotation cycle. The formation of these striations is due to the temperature difference of growth interface in crystal rotation path [17]. Specifically, two main factors could induce the temperature difference: First, the imperfection of mechanical structure can generate the departure of the crystal rotation axis from the thermal center [17,20], which can be reduced but not be eradicated. Moreover, the second point, even in ideal mechanical structure, the asymmetric temperature field still exists. It refers to the eccentric isothermal loop that caused by the imperfect heating element and asymmetric heat-insulation. Furthermore, since the interaction of solid crystal and melt, the asymmetric isothermal has relatively weak effect in growth interface. However, this temperature difference has significant influence on the triple solid-liquid-gas line (growth interface edge) [27], and even could change the crystal diameter. It explains the apparent ravines of rotation striations on crystal surface.

From above discussion, we can conclude that the horizontal temperature difference in crystal rotation path cannot be eliminated. Correspondingly, as seen in Fig. 2a and b, the equal-spaced striations

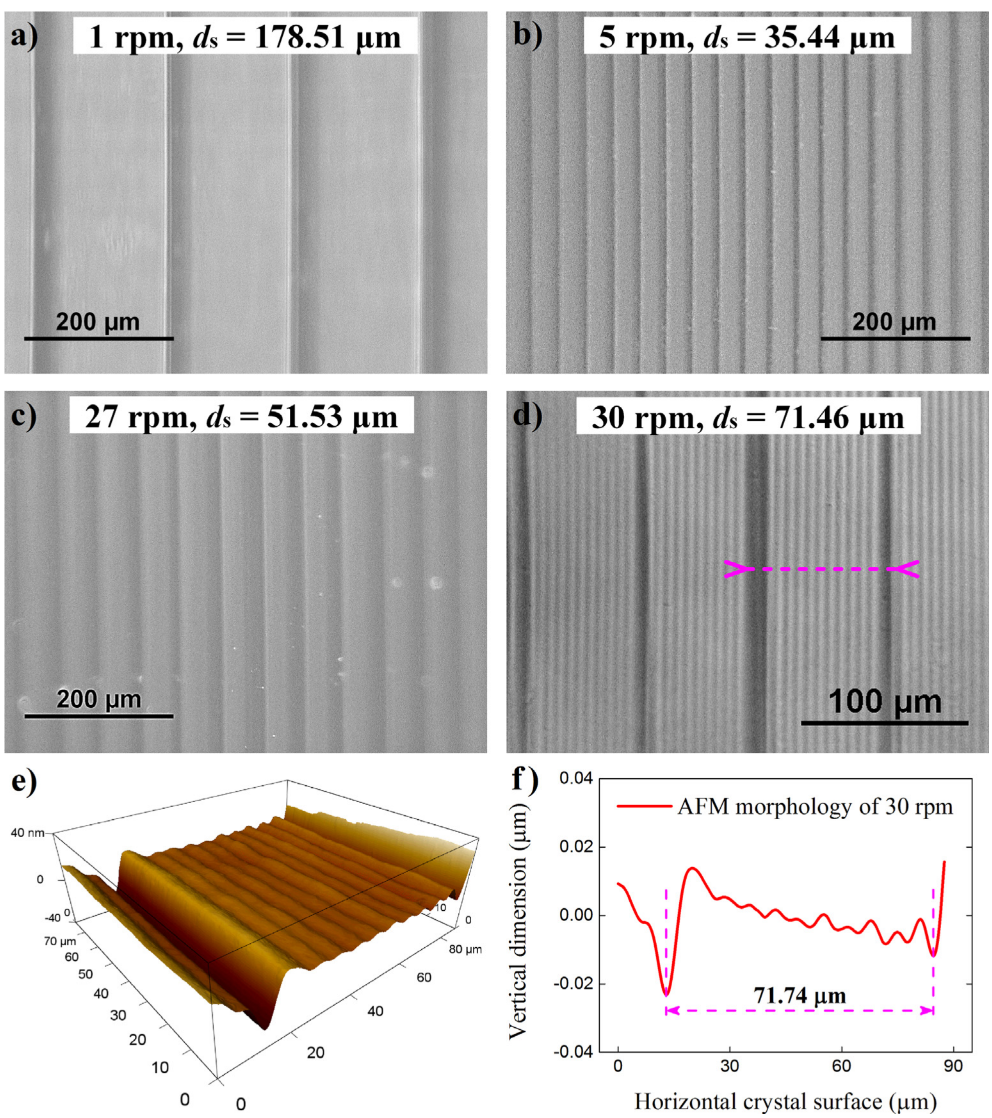

Fig. 2. (a–d) The crystal surface morphologies in different rotation rates of n = 1, 5, 27 and 30 rpm. (e and f) The micro-morphology between two convection striations (n = 30 rpm).

could be observed in crystal surface. The as-grown crystals were obtained in a stable growth system without power fluctuation. During crystal growth, the diameter of the as-grown crystal and the platinum crucible are 20 and 80 mm, respectively, which means the drawdown rate is about one-fifteenth of the pulling rate (10 mm/h). Therefore, under the specific rotation rates of $n = 1$ and 5 rpm, the expected spacing of rotation striations should be 178.20 µm and 35.64 µm, respectively. Thus, combing with the measured striations spacing of 178.51 µm and 35.44 µm in Fig. 2a and b, we can conclude that the practical measurement spacing is consistent with expected result; moreover, the rotation striations are consistent with the actual rotation period ($T_R = 1/n$).

Obviously, besides rotation striations, the eccentric isothermal loop would generate a regular variation of thermoelectric potential which would be reflected in GEMF spectrum as well. The insets of Fig. 3a and b present the original GEMF (O-GEMF) spectra of low rotation rates 1 and 5 rpm, respectively. One can point a strictly periodic oscillation. The GEMF spectra analysis (FFT), as seen in Fig. 3a and b, show the main frequencies of MSA spectra ($f_{R\text{-}GE\text{-}1} = 0.0167$ Hz, $f_{R\text{-}GE\text{-}5} = 0.0836$ Hz). The main frequencies, as expected, are highly consist with the target rotation frequencies of 1 and 5 rpm ($f_{R\text{-}1} = 0.0167$ Hz, $f_{R\text{-}5} = 0.0833$ Hz), respectively. To further clarify, the measured striations spacing from crystal surface (d_S) and the calculated striations spacing from GEMF (d_{GE}) are collected in Table 1 as well. In general, rotation striations and GEMF spectrum are the two types of external appearance of crystal rotation, and are affected by the temperature difference in rotation path. On the basis of the rotation striations in Fig. 2(a, b) and the MSA spectra in Fig. 3(a, b), the in-situ detection of rotation striations is achieved.

3.2. GEMF of convection striations

The oscillatory melt flow is an inherent characteristic in CZ convection system [19], and has a significant effect on the crystallization, crystal shape, concentration field, defect formation and the crystal quality [8,28,29]. However, this common oscillation cannot be observed by neither a thermal couple nor a load cell in conventional CZ furnace. Essentially, the flow pattern is driven by the competition of natural convection (buoyancy and Marangoni convection) and forced convection (crystal rotations) [7,9,30,31]. In normal CZ crystal growth condition, since both Marangoni convection and buoyancy convection flow in the same direction and are generated by temperature difference, it is impossible to distinguish one from the other [32]. Then, we collectively call the two convections as natural convection in the following pages. On the other

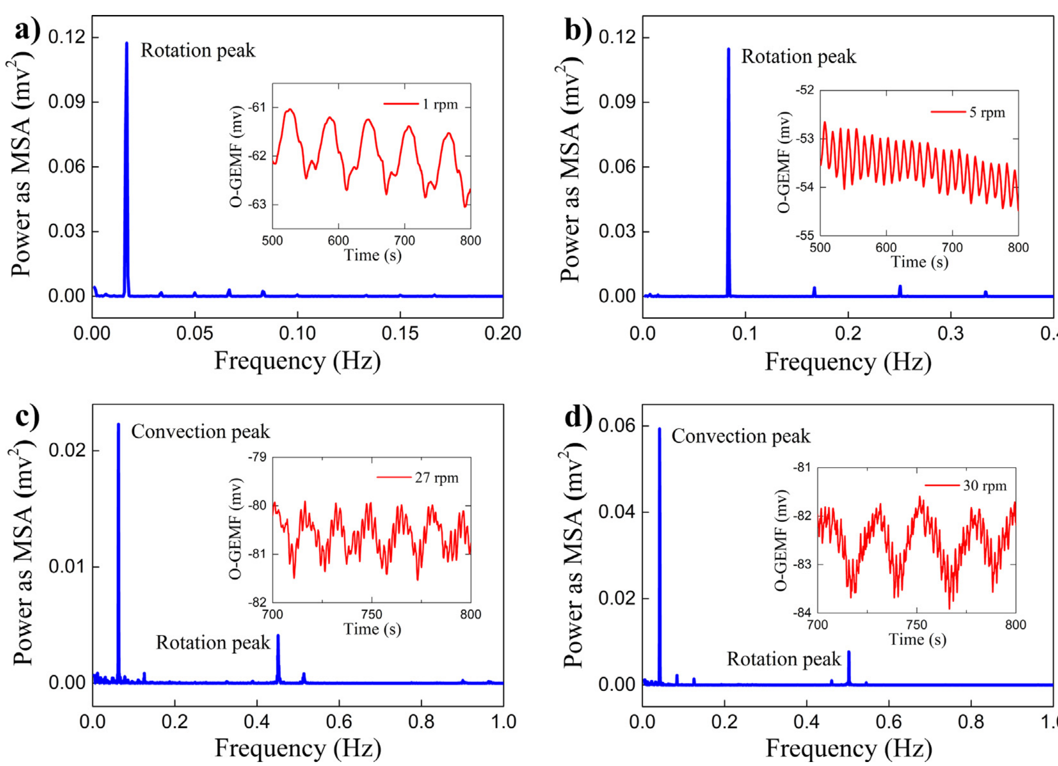

Fig. 3. The FFT spectra of GEMF signals in different rotation rates: $n = 1$ rpm (a), 5 rpm (b), 27 rpm (c) and 30 rpm (d). The insets are the corresponding time-dependent original GEMF (O-GEMF) spectra. From a to d, the calculated rotation frequency in GEMF are $f_{R\text{-}GE} = 0.0167$, 0.0836, 0.4512, 0.5022 Hz, respectively. In c and d, the calculated convection frequency in GEMF are $f_{C\text{-}GE} = 0.0590$ and 0.0418 Hz, respectively.

Table 1
Measured and calculated frequency, period and striations spacing of actual CZ crystals and GEMF spectra in different rotation rates (n).*

n (rpm)	f_R (Hz)	T_R (s)	d_S (µm)	$f_{R\text{-}GE}$ (Hz)	$T_{R\text{-}GE}$ (s)	$f_{C\text{-}GE}$ (Hz)	$T_{C\text{-}GE}$ (s)	d_{GE} (µm)
1	0.0167	60	178.51	0.0167	59.88	–	–	177.84
5	0.0833	12	35.44	0.0836	11.97	–	–	35.55
27	0.0450	2.22	51.53	0.4512	2.22	0.0590	16.95	50.34
30	0.5000	2.00	71.46	0.5022	1.99	0.0418	23.92	71.04

* f_R, T_R and d_S, are obtained from actual growth condition; $f_{R\text{-}GE}$, $T_{R\text{-}GE}$, $f_{C\text{-}GE}$, $T_{C\text{-}GE}$ and d_{GE} are calculated from GEMF spectra.

hand, the forced convection against the natural one, is controlled by the crystal rotation rate. To further investigate the forced convection, Faiez and Rezaei, Munakata and Tanasawa [18,19] have numerically and experimentally demonstrated that, as the crystal rotation rate increases, flow pattern would change from a steady state to an axisymmetric oscillatory state. Specifically, combining our experimental results, in low rotation rates (e.g., 1 and 5 rpm) the natural convection is dominant, the general convection flows form crucible edge to growth interface (inward flow); on the other hand, in high rotation rates (e.g., 27 and 30 rpm) the forced convection is dominant and reverses the general convection (outward flow) [9]. When the forced convection becomes dominant, the balloon shaped cold plume (descending from the edge of rotating crystal) is broke by an upward hot flow periodically [19]. Thus, the periodic flow oscillation is formed, which represents the unstable state of growth interface. Not only that, the periodic flow could oscillate the accurate growth rate in each short period [16,33] and leaves convection striations in crystal surface as well. At the same time, this oscillation phenomenon could be observed in GEMF spectrum.

Under the high rotation rates of 27 and 30 rpm, the convection striations are shown in Fig. 2c and d, and the corresponding O-GEMF spectra are presented in the insets of Fig. 3c and d. Using the similar FFT, the MSA spectra of high rotation rates are presented. Since the MSA spectra of Fig. 3c and d possess similar characteristics of two main peaks, we decide to investigate the data of 30 rpm individually. In 30 rpm, the MSA spectrum possesses two main peaks, as expected, the detected frequency of $f_{R\text{-}GE\text{-}30}$ (0.5022 Hz) coincides with the target rotation frequency ($f_{R\text{-}30}$ = 0 .5 Hz). However, another main frequency of $f_{C\text{-}GE\text{-}30}$ = 0.0418 Hz is brought to our attention. As discussed above, the $f_{C\text{-}GE\text{-}30}$ peak may represent the periodic convection around growth interface. Specifically, it is the outward performance of the convection oscillation induced by crystal rotation. Combing its time period ($T_{C\text{-}GE\text{-}30} = 1/f_{C\text{-}GE\text{-}30}$) of 23.92 s and the integrated pulling rate of 2.97 μm/s (drawdown and pulling rate), the average displacement should be $d_{GE\text{-}30}$ = 71.04 μm. This displacement is highly coincident with the measured striations spacing of $d_{S\text{-}30}$ = 71.46 μm in Fig. 2d. Thus, comparing the measured and calculated frequency, period and striations spacing of actual crystals and GEMF spectra in Table 1, the consistency between d_{GE} and d_S could be regarded as the experimental evidence of precise in-situ detection of convection striations by GEMF spectrum. So far, the convection and rotation frequencies have been revealed with GEMF.

The more interesting work is that, when we further distinguish the GEMF spectrum of convection and rotation frequencies, a remarkable characteristic could be observed. Specifically, on the basis of two main frequencies, the separation result of GEMF spectrum (30 rpm) is presented in Fig. 4a. As seen in Fig. 4a, the red curve (R) and the blue curve (C) represent rotation and convection GEMF signals, respectively. As discussed above, the curve R is mainly affected by the temperature difference in rotation path, and the curve C reflects the convection oscillation in growth interface. Looking back the AFM measurement in the Fig. 2e and f, the fluctuation structure is coincident with the time cycle in curve R (again, it proves the consistency between rotation GEMF and realistic rotation frequency). Moreover, besides the periodic oscillation, curve R possesses the unique characteristic of amplitude variation. More specifically, in Fig. 4a, combining with curve C, the amplitude value (of curve R) is large in the wave trough of curve C, and turns small in the wave crest (of curve C). This phenomenon may be explained by the periodic convection evolution in CZ melt. In growth interface, the forced convection brings hot plume from crucible bottom, and the natural convection brings cold plume from crucible edge [5]. Then, the competition of both convections generates the periodic oscillation of convection and temperature. Based on the GEMF study, in the convection fluctuation line (Fig. 4a, curve C), one can conclude that the enhancement of the absolute value of curve C (the original GEMF value ranges from −81 to −84 mv) implies the upwelling of hot plume (refer to the pink arrow). In this region, the hot plume heightens the temperature of growth interface, and lowers the growth rate, which corresponds to the wave trough of convection GEMF. Such hot plume (in thermal center) could enhance the horizontal temperature gradient of growth interface temporarily. Therefore, the crystal rotation path would suffer higher temperature difference,

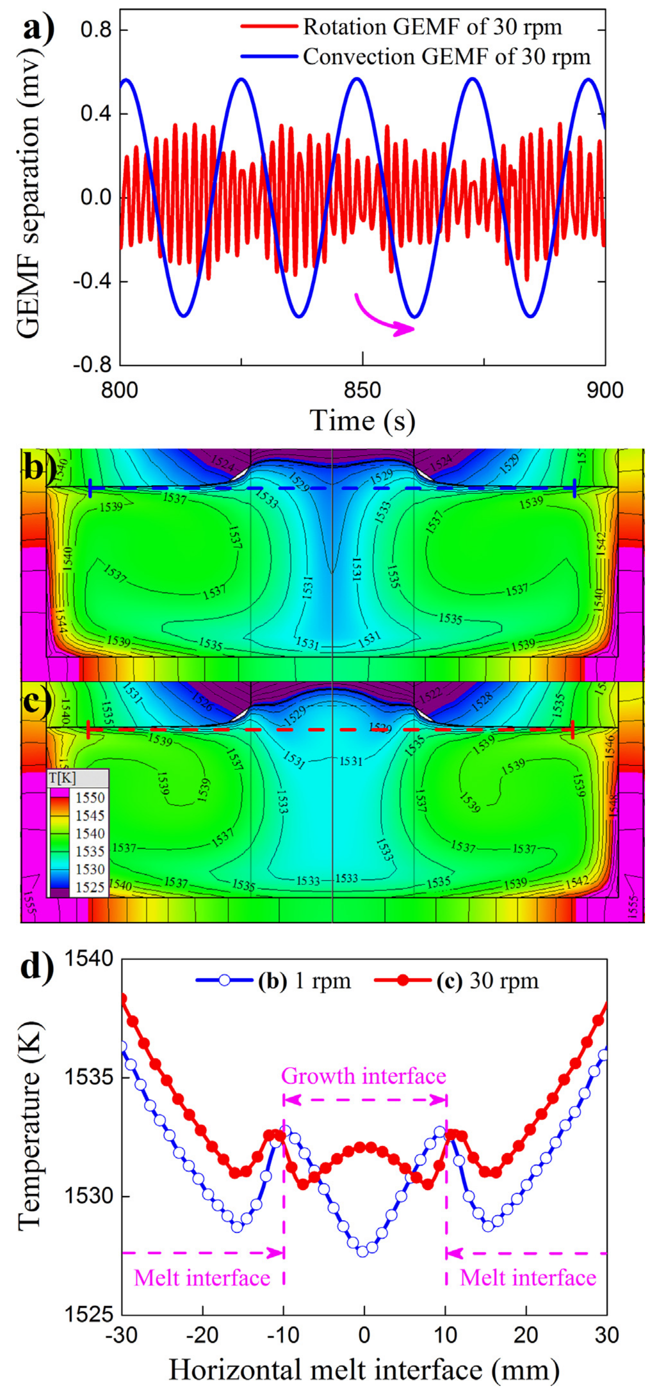

Fig. 4. (a) The separated spectrum of original GEMF signal (n = 30 rpm). (b, c) The simulated temperature fields of CZ melt in the rotation rates of 1 and 30 rpm, respectively. (d) The corresponding melt interface temperature distribution of 1 and 30 rpm.

which in consequence increases the amplitude value of crystal rotation GEMF (curve C).

In addition, considering the above affection of convection to horizontal temperature gradient, the intensity variation of different rotation GEMF could be explained. To be specific, compared with the low rotation rates (1, 5 rpm in Fig. 3a and b), the amplitudes of rotation GEMF turn much smaller in high rotation rates (27, 30 rpm in Fig. 3c and d). Such significant amplitude difference owes to the strong forced convection in high rotation rate. It could be visually explained by the computer simulation results in Fig. 4b and c. Specifically speaking, in the condition of low rotation rate of 1 rpm (Fig. 4b), the convection structure performs unity. Under the combined cooling effect of the solid crystal and the cold plume (natural convection), the strong intraradial temperature gradient is formed. On the other hand, in the condition of high rotation rate of 30 rpm in Fig. 4c, when the forced convection is enhanced, the hot plume against the cold one substantially moderates the temperature gradient in growth interface and weakens the temperature difference in rotation path [34]. The corresponding horizontal temperature fields of liquid interface in low and high rotation rates are presented in Fig. 4d. More intuitively, one can point out that the temperature difference is much smaller in high rotation rate. Then, in consequence, the corresponding intensity of rotation GEMF turns weak.

As discussed in this paper, the periodic convection evolution would oscillate the growth rate, the temperature gradient, and even remelt the as-grown crystal, then leave striations on crystal surface. These variations of rotation and convection cannot be observed by neither a thermal couple nor a load cell. However, the variations are accurately revealed by the GEMF spectrum in real time, and the detection results are strongly proved by the practical crystal surface morphology.

4. Conclusions

After a series of analysis, the close relationship between growth striations and GEMF spectrum has been presented. Specifically, GEMF spectrum presents enough sensitivity to reveal rotation striations, convection striations, and the subtle convection period that used to be studied indirectly. Moreover, the rotation GEMF is mainly affected by the horizontal temperature difference, and the convection one is mainly affected by the complicated periodic melt flow. With the imaging of AFM and stereomicroscopy, the in-situ detection work could be verified by the corresponding regular striations morphology. In general, the GEMF spectrum establishes a real-time feedback of various striations control methods, and offers enough sensitivity to modulate crystal growth condition. Hence, it could become a promising approach to study the striations formation mechanism and optimize the crystal quality.

Acknowledgment

This work was supported by the National Natural Science Foundation of China (NSFC) (Nos. 11372361, 11302268, 11232015, 11472321, 11572355), the National Natural Science Foundation of Guangdong province (2017A030310426), the Guangdong Science & Technology Project (2015B090927005) and the Fundamental Research Funds for the Central Universities (17lgpy37).

References

[1] H.J. Scheel, Theoretical and technological solutions of the striation problem, J. Cryst. Growth 287 (2006) 214–223.
[2] H. Mei, Z. Zeng, Z.H. Qiu, et al., Numerical simulation of crucible rotation in high-temperature solution growth method using a Fourier-Legendre spectral element method, Int. J. Heat Mass Trans. 64 (2013) 882–891.
[3] G.N. Kozhemyakin, Influence of solid-liquid interface shape on striations during CZ InSb single crystal growth in ultrasonic fields, J. Cryst. Growth 360 (2012) 35–37.
[4] K.S. Choe, Growth striations and impurity concentrations in HMCZ silicon crystals, J. Cryst. Growth 262 (2004) 35–39.
[5] J.I. Choi, H.J. Sung, Suppression of temperature oscillation in Czochralski convection by superimposing rotating flows, Int. J. Heat Mass Trans. 40 (1997) 1667–1675.
[6] V. Kumar, B. Basu, S. Enger, et al., Role of Marangoni convection in Si–Czochralski melts—Part II: 3D predictions with crystal rotation, J. Cryst. Growth 255 (2003) 27–39.
[7] A.D.W. Jones, An experimental model of the flow in Czochralski growth, J. Cryst. Growth 61 (1983) 235–244.
[8] T. Shen, C.M. Wu, L. Zhang, et al., Experimental investigation on effects of crystal and crucible rotation on thermal convection in a model Czochralski configuration, J. Cryst. Growth 438 (2016) 55–62.
[9] S.S. Son, K.W. Yi, Experimental study on the effect of crystal and crucible rotations on the thermal and velocity field in a low Prandtl number melt in a large crucible, J. Cryst. Growth 275 (2005) e249–e257.
[10] S. Nakamura, M. Eguchi, T. Azami, et al., Thermal waves of a nonaxisymmetric flow in a Czochralski-type silicon melt, J. Cryst. Growth 207 (1999) 55–61.
[11] H.J. Sung, Y.J. Jung, H. Ozoe, Prediction of transient oscillating flow in Czochralski convection, Int. J. Heat Mass Trans. 38 (1995) 1627–1636.
[12] R. Faiez, Y. Rezaei, Correlation between steady-oscillatory flow transition and the interface inversion process during the Czochralski growth of semitransparent oxide crystal, Jpn. J. Appl. Phys. 55 (2016) 125602.
[13] J.I. Choi, S. Kim, H.J. Sung, et al., Transition flow modes in Czochralski convection, J. Cryst. Growth 180 (1997) 305–314.
[14] Y.Z. Zhu, S.P. Lin, Y. Zheng, et al., Improvement of pyroelectric figures of merit in zirconia-doped congruent lithium niobate single crystals, J. Mater. Sci. 51 (2016) 1–7.
[15] T. Suzuki, Temperature fluctuations in a $LiNbO_3$ melt during crystal growth, J. Cryst. Growth 270 (2004) 511–516.
[16] Y.Z. Zhu, D.C. Ma, S.W. Long, et al., In-situ detection of growth striations by crystallization electromotive force measurement during Czochralski crystal growth, J. Cryst. Growth 475 (2017) 70–76.
[17] B. Cockayne, M.P. Gates, Growth striations in vertically pulled oxide and fluoride single crystals, J. Mater. Sci. 2 (1967) 118–123.
[18] R. Faiez, Y. Rezaei, Rotationally-driven axisymmetric oscillatory convection in a semitransparent Czochralski melt model, J. Cryst. Growth 457 (2017) 72–79.
[19] T. Munakata, I. Tanasawa, Onset of oscillatory flow in a Czochralski growth melt and its suppression by magnetic field, J. Cryst. Growth 106 (1990) 566–576.
[20] P. Hintz, D. Schwabe, Convection in a Czochralski crucible – Part 2: rotating crystal, J. Cryst. Growth 222 (2001) 356–364.
[21] M. Tanaka, M. Hasebe, N. Saito, Pattern transition of temperature distribution at Czochralski silicon melt surface, J. Cryst. Growth 180 (1997) 487–496.
[22] M.T. Santos, J.C. Rojo, A. Cintas, et al., Changes in the solid-liquid interface during the growth of $Bi_{12}SiO_{20}$, $Bi_{12}GeO_{20}$ and $LiNbO_3$ crystals grown by the Czochralski method, J. Cryst. Growth 156 (1995) 413–420.
[23] Y. Kishida, M. Tanaka, H. Esaka, Appearance of a baroclinic wave in Czochralski silicon melt, J. Cryst. Growth 130 (1993) 75–84.
[24] S. Koh, S. Uda, M. Nishida, H. Xinming, Study of the mechanism of crystallization electromotive force during growth of congruent $LiNbO_3$ using a micro-pulling-down method, J. Cryst. Growth 297 (2006) 247–258.
[25] H. Kimura, H. Koizumi, T. Uchida, S. Uda, Influence of impurity doping on the partitioning of intrinsic ionic species during the growth of $LiNbO_3$ crystal from the melt, J. Cryst. Growth 311 (2009) 1553–1558.
[26] Y.Z. Zhu, S.P. Lin, Y. Liu, et al., Efficient synthesis of stoichiometric lithium tantalate powder by a solid-state combustion route, Mate. Manuf. Process. (2015) 1342–1347.
[27] C. Stelian, A. Nehari, I. Lasloudji, et al., Modeling the effect of crystal and crucible rotation on the interface shape in Czochralski growth of piezoelectric langatate crystals, J. Cryst. Growth 475 (2017) 368–377.
[28] L.J. Liu, K. Kakimoto, Effects of crystal rotation rate on the melt-crystal interface of a CZ-Si crystal growth in a transverse magnetic field, J. Cryst. Growth 310 (2008) 306–312.
[29] D. Schwabe, R.R. Sumathi, H. Wilke, An experimental and numerical effort to simulate the interface deflection of YAG, J. Cryst. Growth 265 (2004) 440–452.
[30] R. Teng, Q. Chang, Y. Li, et al., Numerical analysis of solid–liquid interface shape during large-size single crystalline silicon with Czochralski method, Rare Metals (2017) 1–6.
[31] K. Zimik, R.R. Chauhan, R. Kumar, et al., Study on the growth of Nd^{3+}:$Gd_3Ga_5O_{12}$, (Nd:GGG) crystal by the Czochralski technique under different gas flow rates and using different crucible sizes for flat interface growth, J. Cryst. Growth 363 (2013) 76–79.
[32] A. Hirata, M. Tachibana, T. Sugimoto, et al., Control of crystal–melt interface shape during growth of lithium niobate single crystal, J. Cryst. Growth 131 (1993) 145–152.
[33] C. Stelian, T. Duffar, J.L. Santailler, I. Nicoara, Influence of temperature oscillations on the interface velocity during Bridgman crystal growth, J. Cryst. Growth 237 (2002) 1701–1706.
[34] S.S. Son, K.W. Yi, Characteristics of thermal fluctuation in a low Pr, number melt at a large crucible for Czochralski crystal growth method, J. Cryst. Growth 275 (2005) e259–e264.